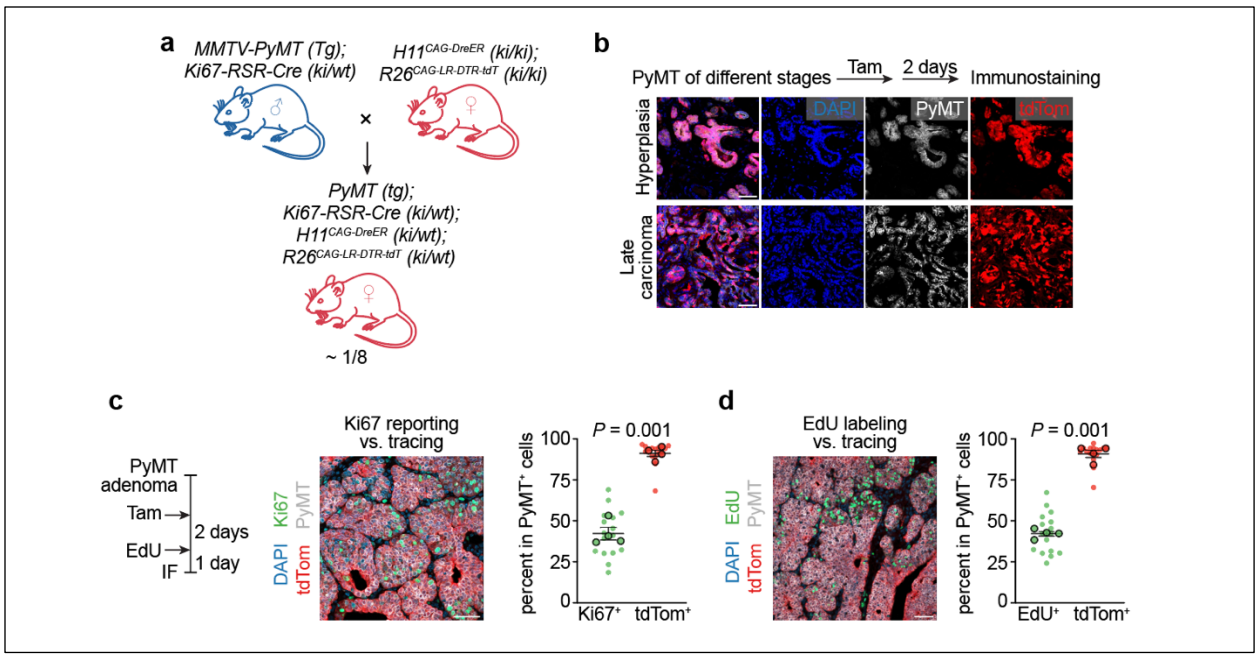

Supplementary Figure 1. Establishment of the PyMT proliferation tracing and deleting system

a). Mating strategy for generating PyMT proliferation tracing and deleting mice (*Tg*, hemizygous transgene; *ki*, knock-in; *wt*, wild-type). One-eighth of the offspring with the desired genotype combination were used for the experiments.

b). Immunostaining for PyMT and tdTomato on PyMT hyperplasia (pre-malignant) sections and late carcinoma sections, assessed two days post-tamoxifen (Tam) treatment (scale bar, 50 μm).

c,d). Comparison of immunostaining for Ki67 (**c**) or EdU labeling (**d**) and genetic fate mapping of Ki67 in PyMT adenoma (scale bar, 50 μm).

Mean ± s.e.m. shown. *P* values were calculated by comparing individual animals using two-tailed paired (**c**,**d**) Student's *t*-test.

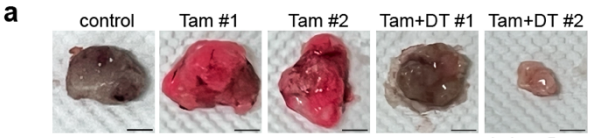

c

Sample	HashTag	non-immune	immune
Tam #1	A0305	2378	2812
Tam #2	A0306	1757	3547
Tam+DT #1	A0307	728	4311
Tam+DT #2	A0308	914	445

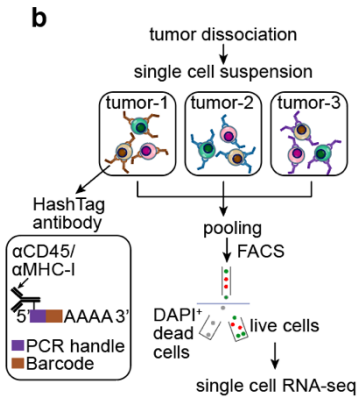

Supplementary Figure 2. Cell hashing for pooled scRNA-seq

a). Macroscopic images of tumor specimens analyzed by scRNA-seq: untreated control tumor (mouse not treated with Tam), primary tumors from Tam-treated mice, and relapsed tumors from mice treated with both Tam and DT (scale bar, 5 mm).

b). Experimental workflow for multiplexed scRNA-seq. Cells were incubated with mixtures of two monoclonal antibodies: anti-CD45 and anti-MHC class I, which are conjugated with identical oligonucleotides (barcode). The anti-CD45 antibodies label immune cells, whereas the anti-MHC class I antibodies label both hematopoietic and non-hematopoietic cells. Single-cell suspensions from various tumor samples were labeled with hashtag antibodies that are conjugated with distinct barcodes, facilitating the identification of the origin of the single-cell transcriptomes. Dead cells were excluded by DAPI staining prior to fluorescent-activated cell sorting (FACS).

c). Cell yield quantification after hashtag-based sample deconvolution.

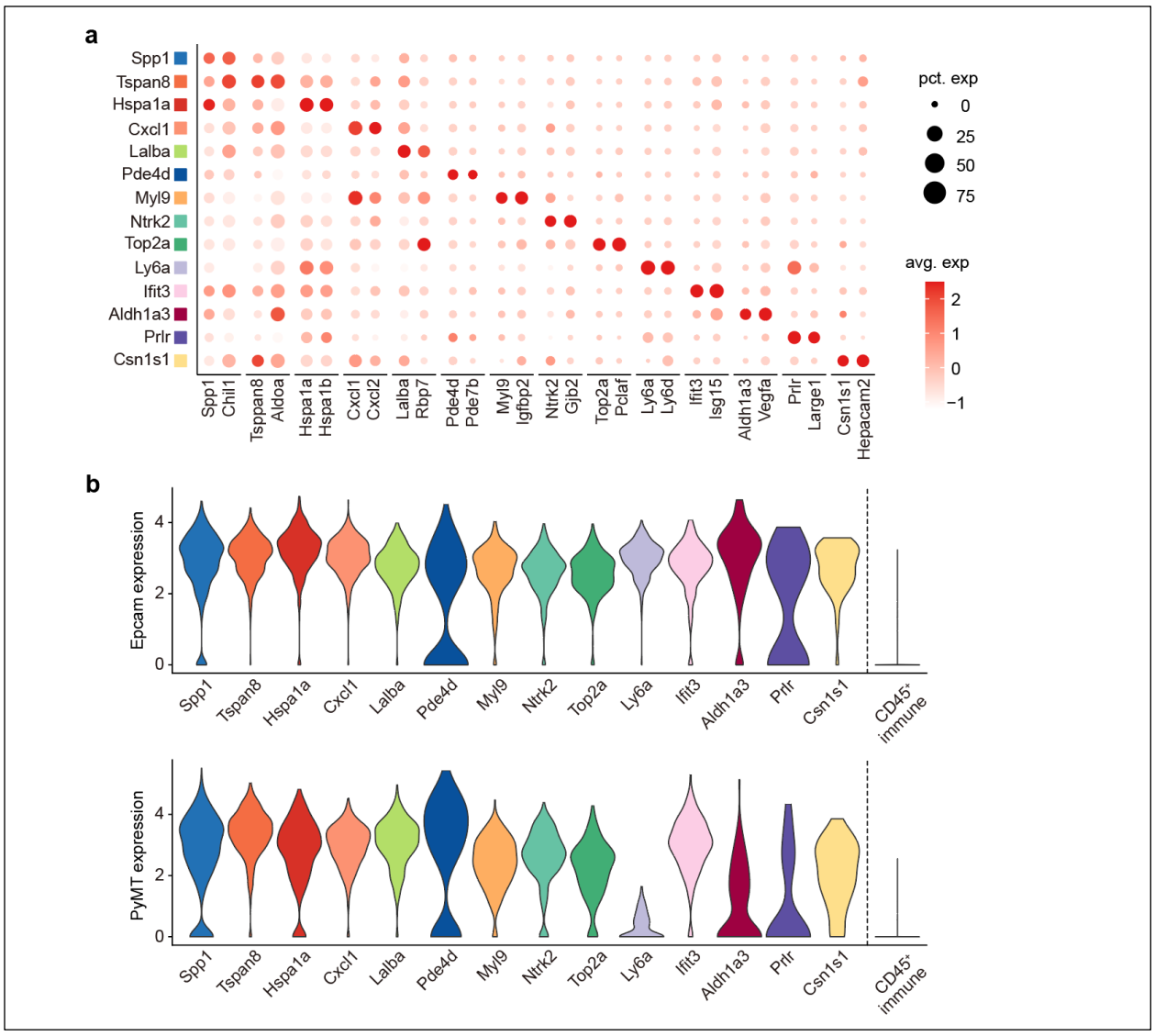

Supplementary Figure 3. Markers for re-clustering and annotating epithelial cells

a). Dot plot showing canonical marker genes for annotating different subsets of epithelial cells. The size of each dot is proportional to the fraction of cells expressing specific genes, while the color intensity reflects the relative expression levels of these genes.

b). Violin plot showing the expression of Epcam, the pan-epithelial cell marker, alongside the expression of oncogenic transgene PyMT. $CD45^{+}$ immune cells served as a negative control. The $Ly6a^{+}$ cluster was classified as normal epithelial cells, due to its low expression of PyMT. Colors as in (**a**).

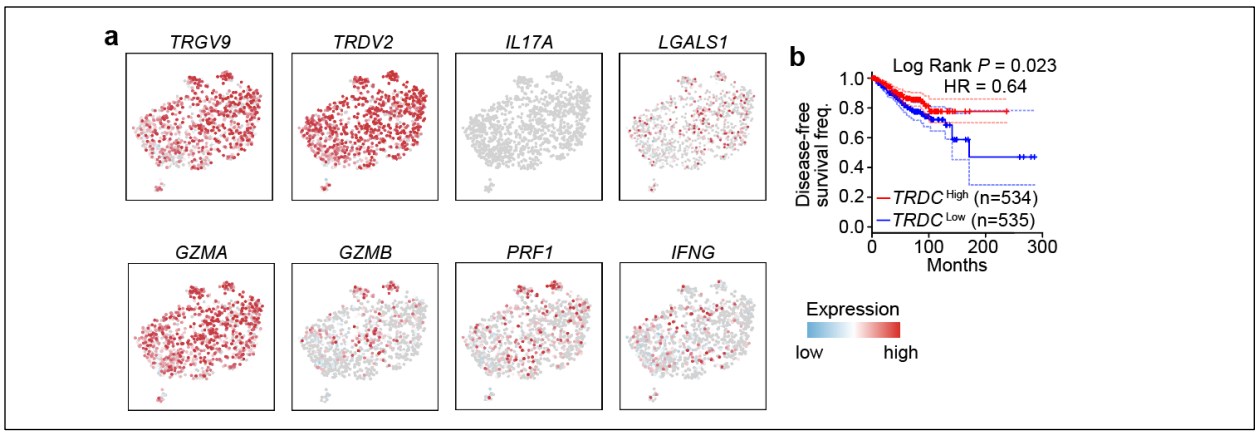

Supplementary Figure 4. γδ T cells in human breast cancer

a). Feature plot visualization of immunosuppressive genes (*IL17A*, *LGALS1*) and pro-inflammatory genes (*GZMA*, *GZMB*, *PRF1*, *IFNG*) in scRNA-seq of human breast cancer dataset.

b). Clinical correlation of γδ T cell infiltration in TCGA breast cancer dataset. The expression of T Cell Receptor Delta Constant (*TRDC*) was used to estimate the abundance of tumor-infiltrating γδ T cells. Kaplan-Meier survival analysis generated via GEPIA2 (http://gepia2.cancer-pku.cn) comparing patients with high versus low *TRDC* expression (log-rank test *P* value shown).

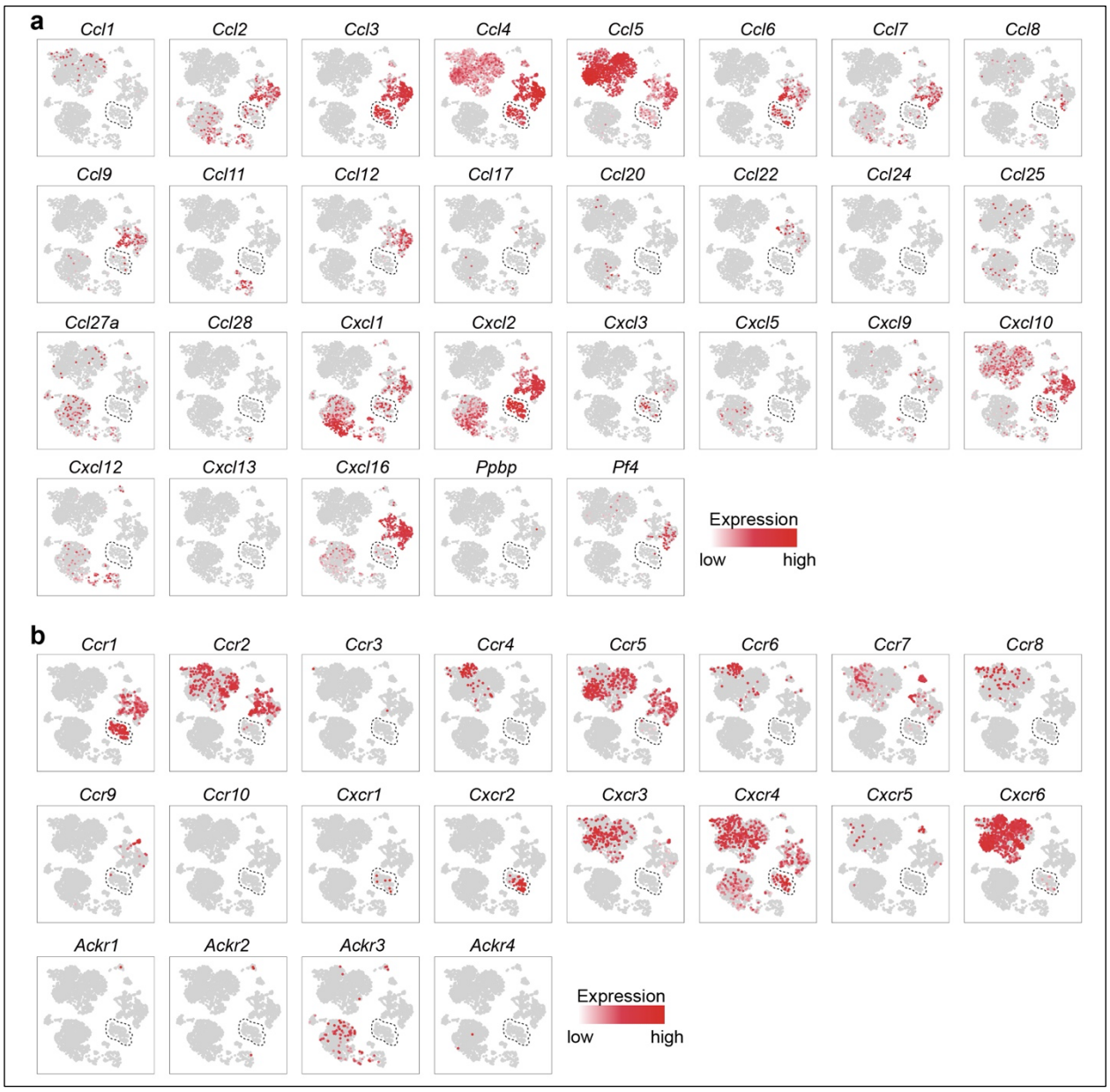

Supplementary Figure 5. Chemokine signaling landscape in the tumor microenvironment a,b). Feature plots showing the expression of chemokines (**a**) and corresponding receptors (**b**). Dashed lines highlight neutrophils as the exclusive Cxcr2^{+} population. The UMAP visualization of cell composition is as in **Fig. 2**.

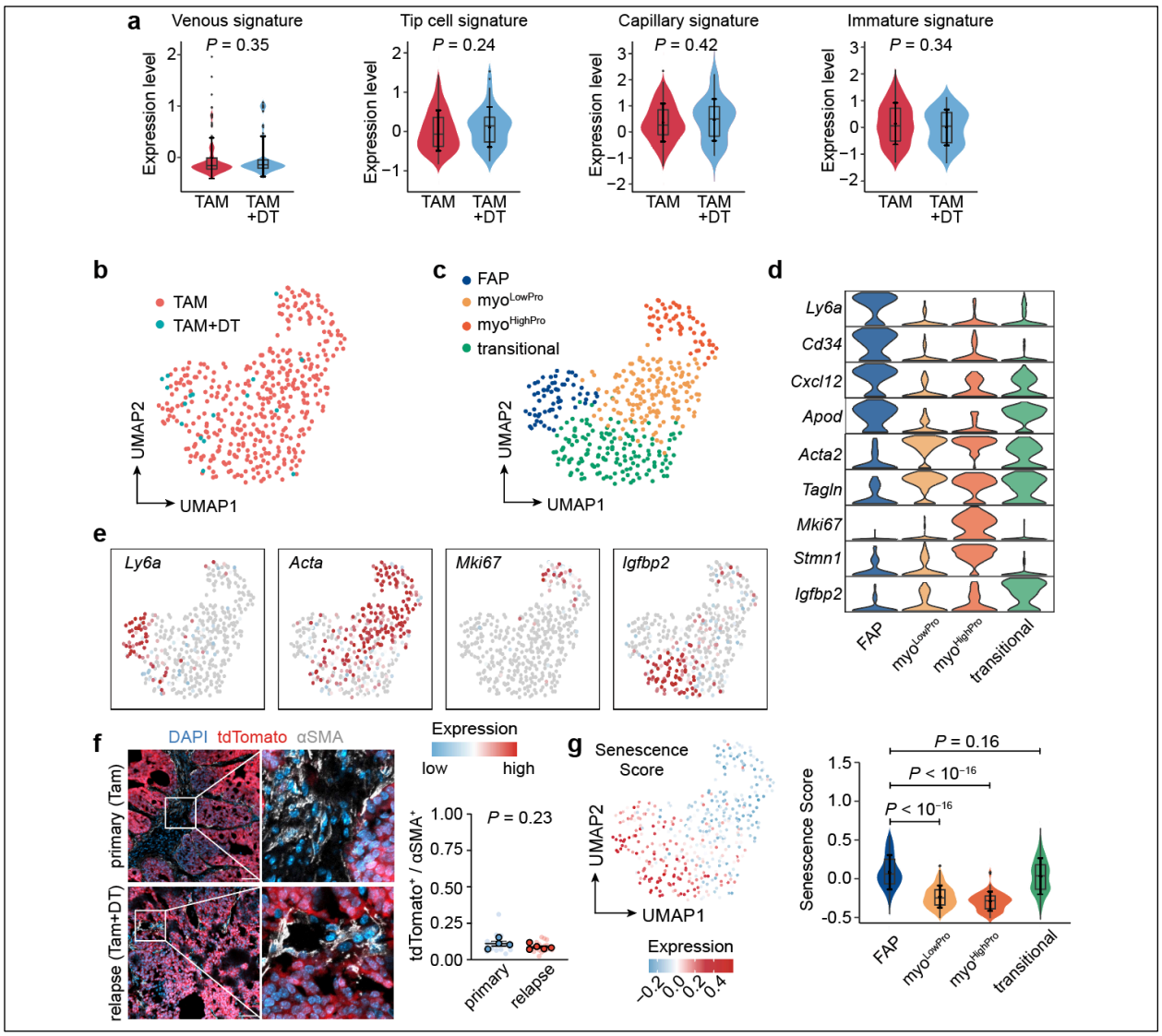

Supplementary Figure 6. Endothelial cells and fibroblasts in PyMT tumor relapse

a). Violin plots comparing four different vascular signatures in endothelial cells isolated from primary and relapsed tumors.

b,c). UMAP visualization of fibroblast populations in primary (Tam) and relapsed tumor (Tam+DT) (**b**) and heterogeneity of fibroblasts (**c**).

d,e). Violin plots (**d**) and feature plots (**e**) showing markers associated with each fibroblast subset.

f). Proliferative capacity assessment by tdTomato^{+} fibroblast quantification (scale, 50 μm).

g). Cellular senescence evaluation across fibroblast subtypes. Box plots show median (center line), IQR (box bounds), and 1.5×IQR (whiskers).

Mean ± s.e.m. shown. The *P* values were calculated using two-tailed paired Mann-Whitney *U*-test (**a**, **f**, **g**).